PROCEEDINGS OF SCIENCE

Modelling Gradual Solar Energetic Particle Events Using the SEPCaster Model

Gang Li,[a,*] **Meng Jin**[b] **and Zheyi Ding**[c]

[a] *Department of Space Sciences, University of Alabama in Huntsville, Huntsville, AL, USA*

[b] *Lockheed Martin Solar & Astrophysics Laboratory, Palo Alto, CA, USA*

[c] *Centre for mathematical Plasma Astrophysics, KU Leuven, 3001 Leuven, Belgium*

E-mail: gangli.uahuntsville@gmail.com

Solar energetic particle events is a major concern of Space Weather. We develop a SEPCaster model to simulate the acceleration and transport of solar energetic particles in gradual SEP events. SEPCaster combines the AWSoM and the iPATH codes with the AWSoM code providing a physical description of the solar wind and the coronal mass ejection (CME), and the iPATH code treating the acceleration and transport of energetic particles. Using SEPCaster, we investigate particle acceleration when the CME-driven shocks are still close to the Sun and obtain reasonable agreements between our simulation and observations for individual events, at multiple spacecraft. By varying the model parameters, we identify important parameters that control the production of energetic ions in large SEP events.

38th International Cosmic Ray Conference (ICRC2023)
26 July - 3 August, 2023
Nagoya, Japan

ICRC2023
38th International Cosmic Ray Conference
The Astroparticle Physics Conference

*Speaker

PoS(ICRC2023)1314

1. Introduction

Coronal mass ejections (CMEs) are a major concern of space weather. In large CMEs, considerable coronal material can be ejected with energies reaching 10^{31-32} ergs. The fast-moving ejected coronal material can produce shock waves in front of the CME. These shocks can accelerate ions to several GeV per nucleon [1] and because of this, CME-driven shocks are often regarded as the major sites for the acceleration of Solar Energetic Particles (SEPs).

The underlying acceleration mechanism at CME-driven shocks is believed to be diffusive shock acceleration (DSA), also known as first-order Fermi acceleration. DSA was proposed to explain the acceleration of galactic cosmic rays in supernova shocks. An earlier attempt of applying the DSA to interplanetary shocks by Lee [2] solved the coupled particle transport and upstream Alfvén wave intensity equations. The work of Lee [2] was extended by Gordon et al. [3]. In [3], the authors compared the steady state solutions of energetic particles and the upstream wave spectra with observations at Earth's bow shock. The steady state solutions by Gordon et al. [3] were appropriate since the bow shock is stationary. For a propagating CME-driven shock, however, the shock parameters and the solar wind plasma vary with the heliocentric distance. Consequently the problem of particle acceleration in SEP events is intrinsically time-dependent and thus more difficult, and a sophisticated model is needed.

Many models have been developed to study SEPs. In the work of Zank et al. [4], the authors adopted the steady-state DSA solution by [3] at a series of times, but constrained the maximum particle energy at these times by balancing the shock dynamic time scale with the particle acceleration time scale. The shock is followed numerically using the ZEUS MHD code. Accelerated particles are followed in an onion-shell model behind the shock and those that escape upstream of the shock are followed assuming a ballistic propagation. This work has been further extended by Rice et al. [5], Li et al. [6] and was the foundation of the Particle Acceleration and Transport (PATH) model. Extending the PATH model to a 2D geometry has been done by Hu et al. [7], leading to the iPATH 2D model. The model still relies on a 2D ZEUS MHD code to provide the background solar wind and the CME-driven shock. This means that the iPATH model does not contain a realistic description of the background solar wind, nor does it contain a physical description of the CME eruption. The SEPCaster model we discuss here addresses both issues.

2. The SEPCaster Model

SEPCaster is based on two state-of-the-art research models: 1) the AWSoM model which follows the initiation and propagation of a fast CME, and 2) the iPATH model which follows the acceleration of solar energetic particles at the CME-driven shock front and their subsequent transport in the solar wind.

Both models are widely used in the heliospheric physics research community and have been delivered to the Community Coordinated Modeling Center (CCMC), allowing users to use them for different purposes. AWSoM is available via CCMC's Runs-on-Request system, and iPATH is currently in the model onboarding process and will become available to users soon.

Figure 1 is a flowchart of the SEPCaster model. SEPCaster will run in two different modes: An automatic forecasting mode and a user interactive mode. When running in the automatic

forecasting mode, the SEPCaster requires minimum user inputs, and will produce a forecast of SEP in the format of time intensity profile and particle energy spectra for both protons and heavy ions (Carbon, Oxygen and Iron, etc). The input of the model is real-time magnetogram, which will be fetched automatically through https://www.lmsal.com/forecast. Because the magnetogram is updated every 6 hours, SEPcaster will also be updated with a 6-hour interval. In this mode, SEPCaster runs in a continuous fashion. The output data can be saved in a user specified format and stored for 24 hours. The automatic forecasting mode is the nominal mode of SEPCaster. The user interface in this mode is designed to be as simple as possible.

The second mode of the SEPCaster is the user-interactive mode. When running in this mode, users have the extra flexibility to examine the radiation environment at points of interest for current or a past SEP event by modifying and fine-tuning the input data. This mode can be particularly useful for an in-depth examination of a past event. The designing philosophy of the user interface for this mode is to provide the users an interactive environment where the users are prompted with a series of menus for input parameters. The interactive nature of such a user interface makes it easy to explore the SEPCaster capability, while at the same time it ensures the user-modified input data physically meaningful. The user interfaces for these two different modes are illustrated in the green box at the upper part of Figure 1. The left (right) is for the automatic forecast (user interactive) mode. The magnetogram of the entire visible solar surface is shown, with individual active regions labelled. When individual ARs are chosen by placing the mouse cursor on it, a side window will pop up showing a magnetic flux rope configuration using the Gibson-Low (GL) prescription. In the user-interactive mode, the same magnetogram will be shown. Different from the automatic forecast mode, when an AR is chosen, a pop-up menu will appear with choices for relevant parameters that can be used to construct the flux rope and the CME eruption. Users can change these values, and drive the SEPCaster accordingly.

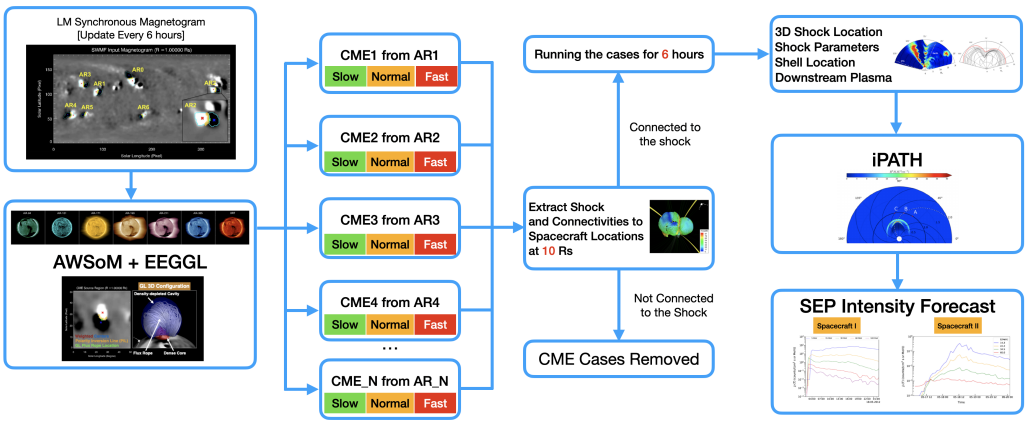

Figure 1: Flowchart of the SEPCaster. SEPCaster will run in two different modes: an automatic forecasting mode and a user interactive mode. In the automatic mode, the model will provide a continuous, 24X7 forecast of SEPs with a 24-hour lead time, updating every 6 hours. In the user-interactive mode, users can modify the inputs to drive the SEPCaster to examine particular events of interests.

2.1 Modelling the Background Solar Wind and CME with AWSoM

The Alfvén Wave Solar Model (AWSoM) is a data-driven global MHD model within Space Weather Modeling Framework (SWMF: Tóth et al. 8). The simulation domain extends from the upper chromosphere to the corona and heliosphere beyond the Mars orbit [11]. The inner boundary conditions for electron and proton temperatures T_e and T_i and number density n are assumed at $T_e = T_i = 50{,}000$ K and $n = 2{\times}10^{17}$ m^{-3}, respectively. This density at the inner boundary allows chromospheric evaporation to self-consistently populate the corona with an appropriately high density, as found on the Sun. The inner boundary density and temperature do not otherwise have a significant influence on the global solution [12]. The inner boundary condition of the magnetic field can be specified by magnetic field observations. For this project, we will adapt the Lockheed Martin surface flux transport model based synchronous magnetogram [13] which assimilates new observational data every 6 hours. Aflvén waves are driven at the inner boundary with a Poynting flux that scales with the surface magnetic field. The solar wind is heated by Alfvén wave dissipation and accelerated by thermal and Aflvén wave pressure. Electron heat conduction (both collisional and collisionless) and radiative cooling are also included in the model. In addition, the electron and proton temperatures are treated separately, a feature that has been shown to be critical for reproducing physically correct CME-driven shocks [14]. By a physically consistent treatment of wave reflection, dissipation, and heat partitioning between the electrons and protons, the AWSoM has been demonstrated to reproduce high-fidelity global solar corona conditions (e.g., Sokolov et al. 15, Jin et al. 16).

To generate a CME eruption, a simulation tool Eruptive Event Generator Gibson-Low (EEGGL; Jin et al. 17) that inserts a Gibson-Low (GL) flux rope [10] and automatically determines the Gibson-Low flux rope parameters through a handful of observational quantities (i.e., magnetogram and CME speeds) so that the modeled CMEs can propagate with the desired CME speeds near the Sun. Analytical profiles of the GL flux rope are obtained by finding a solution to the magnetohydrostatic equation $(\nabla \times \mathbf{B}) \times \mathbf{B} - \nabla p - \rho \mathbf{g} = 0$ and the solenoidal condition $\nabla \cdot \mathbf{B} = 0$. This solution is derived by applying a mathematical stretching transformation to an axisymmetric spherical ball of twisted magnetic flux in the pressure equilibrium. The transformed flux rope appears as a tear-drop shape of twisted magnetic flux. At the same time, Lorentz forces are introduced, which leads to a density-depleted cavity in the upper portion and a dense core at the lower portion of the flux rope. This flux rope structure helps to reproduce the 3-part density structure of the CME in the observation [18]. The GL flux rope and contained plasma are then superposed onto the steady-state solar corona solution: i.e. $\rho = \rho_0 + \rho_{\rm GL}$, $\mathbf{B} = \mathbf{B_0} + \mathbf{B}_{\rm GL}$, $p = p_0 + p_{\rm GL}$. The combined background-flux rope system is in a state of force imbalance, and thus erupts immediately when the simulation is advanced forward in time.

2.2 Modelling the Acceleration and Transport of SEPs using iPATH

In SEPCaster we follow the iPATH model to examine the acceleration of particles at the CME-driven shock and their subsequent transport in the solar wind. The iPATH model follows SEPs in the ecliptic plane, thus a 2D model. This is extended to 3D in SEPCaster. Plasma parameters of the background solar wind and the shock are provided by the AWSoM model and the coupling between the two codes is explained in section 2.3.

Using these parameters iPATH computes the accelerated particle spectra at the shock front assuming DSA as the acceleration mechanism. Accelerated particles can convect with the shock downstream of the shock. Such a convection is followed using a 3D shell in SEPCaster. Accelerated particles convect with the shock and diffuse among different cells. Once particles diffuse far enough upstream of the shock, they can escape from the shock complex. In iPATH the propagation of these particles in the solar wind, along and across the background interplanetary magnetic field, is followed using a backward stochastic differential equation method. The cross-field diffusion is easily included in this approach [7]. Since the upstream solar wind is unperturbed, we approximate the upstream solar wind magnetic field by a nominal Parker field in the transport module. The particle flux at a given location $\mathbf{r}$ and a given time t is obtained.

Once particles escape from the shock complex, they propagate along the IMF in the relatively undisturbed solar wind. Their propagation is described by the focused transport equation where the particle pitch angle experiences magnetic focusing and diffusion.

2.3 Coupling between AWSoM and iPATH

To compute the accelerated particle spectra at the shock front, the SEPCaster model requires the knowledge of a number of plasma parameters for the entire downstream behind the shock front. These parameters are provided by the AWSoM code. Because the AWSoM follows the CME since its eruption, particle acceleration below $10R_s$ is naturally included in the SEPCaster, unlike the 1D PATH and 2D iPATH models.

The coupling is achieved through the following steps: the iPATH code will query the AWSoM code output at a series of time steps, with a default interval of half an hour. The accelerated particle spectra are computed at these times at the shock front. In response to the query, the AWSoM output will return a datacube consisting the current shells behind the shock and the plasma parameters within these shells. These shells are of 3D in geometry, consisting of multiple cells. These plasma parameters include number density, solar wind speed and magnetic field. Based on these plasma parameters and the shock location at the previous time step, SEPCaster will generate a new shell behind the shock, and energetic particles will be followed to diffuse among all previous shells and the newly generated shell. As the number of shells increases over time, the amount of data in the datacube also increases. Note that to be able to follow energetic particles downstream of the shock, all shells constructed earlier have to be identified and tracked in the AWSoM code.

3. An event study

Using the philosophy of SEPCaster, we have examined the 2012 May 17 GLE event. Figure 2 is the 3D shock morphology and various shock parameters at $t = 60$ minutes obtained from the AWSoM code. The four panels are for four different shock parameters. They are the compression ratio, the shock speed, the shock Alfvén Mach number, and the angle $\theta_{\rm BN}$ between the upstream magnetic field and the shock normal. Also shown in the figure are field lines that connect to the Earth, STA, and STB, respectively. As we can see from the figure, at this time the earth is connected to a region with a large compression ratio, implying a more efficient particle acceleration. In comparison, STA is connected to a region with a smaller compression ratio. Note that for the two distinct shock surfaces, the one moving faster (at the left of the Figure connecting to STA) results in

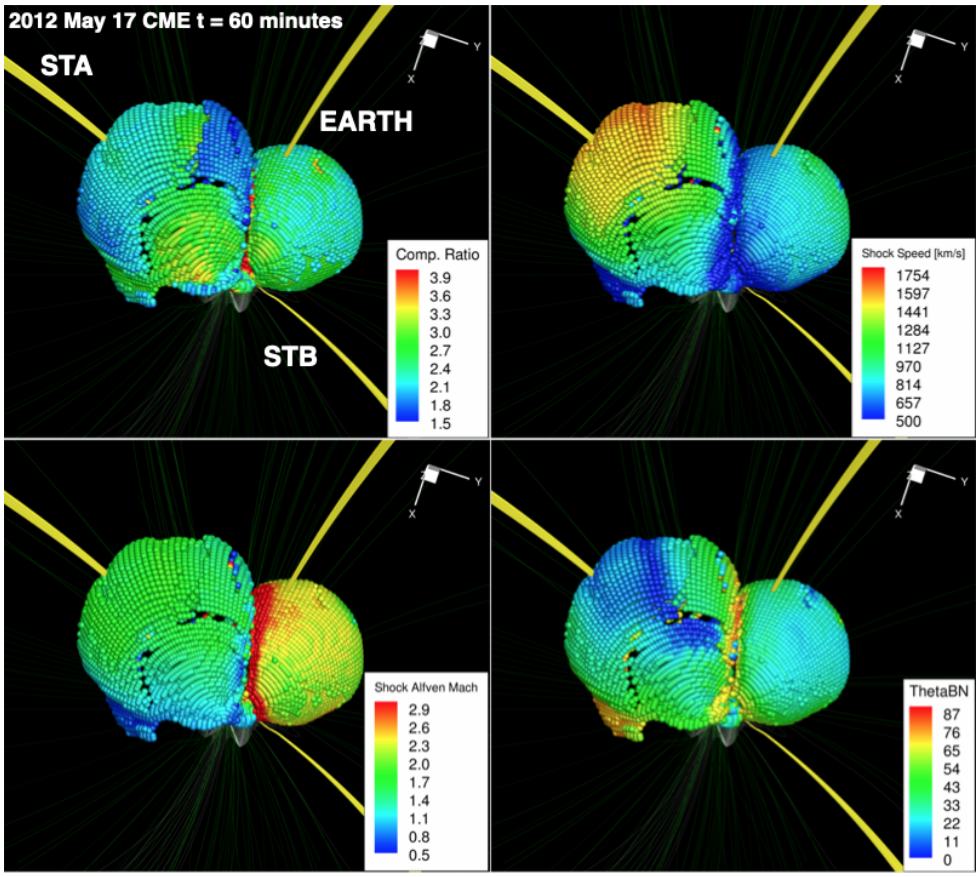

Figure 2: CME-driven Shock surface showing the shock compression ratio, shock speed, shock Alfvén Mach number, and shock θ_{Bn} at$t$ = 60 minutes. The yellow lines are magnetic field lines that connect to the Earth, STB, and STA, respectively. Adapted from [19].

a weaker shock (as shown by the smaller compression ratio and Mach number), which demonstrates the importance of considering the inhomogeneous background solar wind where shocks propagate.

Figure 3 plots the 24-hour spectra at energies above 80 MeV at the Earth. The black curve shows the observation from PAMELA [9] and the red curve the model results. For the simulation, a 15% uncertainty for the intensity is assumed to represent model uncertainty due to, e.g., magnetic connection, solar wind speed, magnetic field strength, etc. This model uncertainty yields a similar value to the observation at ~ 100 MeV. Fitting both spectra by the functional form

$$\Phi(E) \propto E^{-\gamma} exp\,(-E/E_r) \tag{1}$$

yields the spectral indices to be $\gamma = 2.42 \pm 0.14$ for PAMELA observation and $\gamma = 2.51 \pm 0.13$ for the simulation; and the roll-over energy to be $E_r = 498.7 \pm 116.2$ MeV for PAMELA observation and $E_r = 440.7 \pm 72.6$ MeV for the simulation. The simulated spectral indices and the break energies agree very well with those observed. Note that at these energies, particles are accelerated early in the event when the shock is still below $10R_s$. Therefore the usage of the AWSoM code is crucial as it provides the shock profiles as low as $\sim 2R_s$.

One notable feature of SEPCaster is its capability to obtain results at multiple locations. Figure 4

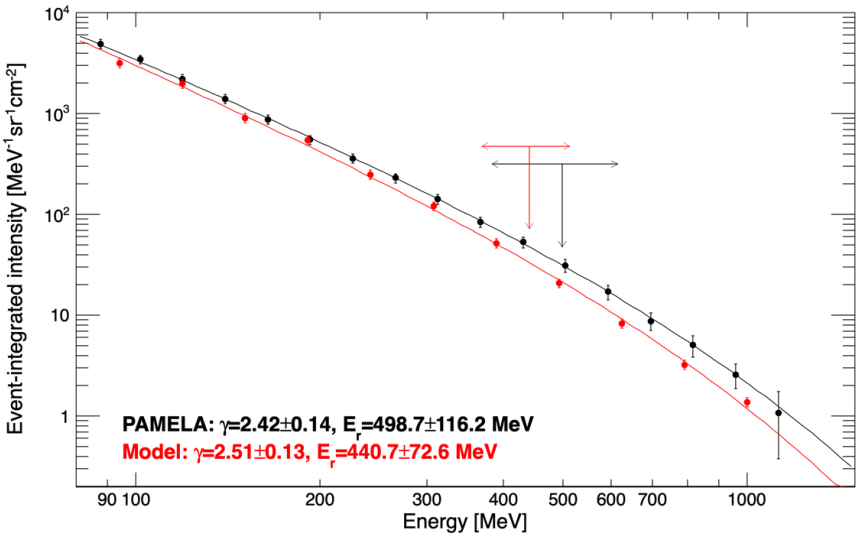

Figure 3: Spectrum comparison between PAMELA observation and model simulation. The roll-over feature at high energy can be seen in both the observation and the simulation. The fitted parameters correspond to an Ellison-Ramaty spectral fitting. The black and red arrows indicated the location of the roll-over energies with the uncertainty indicated by the horizontal bars. Adapted from [19].

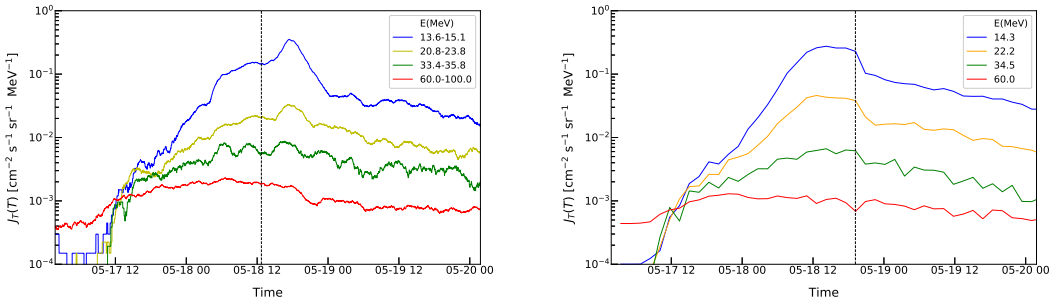

Figure 4: Left: time profiles of protons for 4 energy bins as observed by STEREO-A; Right: model calculations from AWSoM+iPATH. The vertical dashed lines mark the shock arrival from observation and the model calculation. Adapted from [19].

shows the observed (left) and modelled (right) time profiles at the location of STA spacecraft. The 4 energy bands from observations are 13.6-15.1 MeV, 20.8-23.8 MeV, 33.4-35.8 MeV, 60-100 MeV, respectively. The simulation results are for 14.3 MeV, 22.2 MeV, 34.5 MeV and 60 MeV. The observed shock arrival time at STA was around 12:43 local time on 2012/5/18 and the modelled shock arrival time is 6.5 hours later. This difference is small. Furthermore, the simulated time profiles agree reasonably well with the observation.

References

[1] Mewaldt, R. A. 2006, Space Science Reviews, 124, 303.

[2] Lee, M. 1983, Journal of Geophysical Research (Space Physics), 88, 6109.

[3] Gordon, B. E., Lee, M. A., Möbius, E., & Trattner, K. J. 1999, Journal of Geophysical Research: Space Physics, 104, 28263.

[4] Zank, G., Rice, W. K. M., & Wu, C. 2000, Journal of Geophysical Research: Space Physics, 105, 25079.

[5] Rice, W. K. M., Zank, G. P., & Li, G. 2003, Journal of Geophysical Research: Space Physics, 108, 1.

[6] Li, G., Zank, G. P., & Rice, W. K. M. 2003, Journal of Geophysical Research: Space Physics, 108, 1.

[7] Hu, J., Li, G., Ao, X., Zank, G. P., & Verkhoglyadova, O. 2017, Journal of Geophysical Research (Space Physics), 122, 10,938.

[8] Tóth, G., van der Holst, B., Sokolov, I. V., et al. 2012, Journal of Computational Physics, 231, 870.

[9] Bruno, A., Bazilevskaya, G. A., Boezio, M., et al. 2018, ApJ, 862, 97.

[10] Gibson, S. E., & Low, B. C. 1998, ApJ, 493, 460.

[11] van der Holst, B., Sokolov, I. V., Meng, X., et al. 2014, ApJ, 782, 81.

[12] Lionello, R., Linker, J. A., & Mikić, Z. 2009, ApJ, 690, 902.

[13] Schrijver, C. J., & DeRosa, M. L. 2003, Solar Physics, 212, 165.

[14] —. 2013, ApJ, 773, 50.

[15] Sokolov, I. V., van der Holst, B., Oran, R., et al. 2013, ApJ, 764, 23.

[16] Jin, M., Manchester, W. B., van der Holst, B., et al. 2017, ApJ, 834, 172.

[17] —. 2017, ApJ, 834, 173.

[18] Illing, R. M. E., & Hundhausen, A. J. 1985, Journal of Geophysical Research (Space Physics), 90, 275.

[19] Li, G., Jin, M., Ding, Z., et al. 2021, ApJ, 919, 146.